Review article **Open Access**

Gitanjal Deka, Chi-Kuang Sun, Katsumasa Fujita and Shi-Wei Chu*

Nonlinear plasmonic imaging techniques and their biological applications

DOI 10.1515/nanoph-2015-0149
Received December 1, 2015; revised January 31, 2016; accepted February 14, 2016

Abstract: Nonlinear optics, when combined with microscopy, is known to provide advantages including novel contrast, deep tissue observation, and minimal invasiveness. In addition, special nonlinearities, such as switch on/off and saturation, can enhance the spatial resolution below the diffraction limit, revolutionizing the field of optical microscopy. These nonlinear imaging techniques are extremely useful for biological studies on various scales from molecules to cells to tissues. Nevertheless, in most cases, nonlinear optical interaction requires strong illumination, typically at least gigawatts per square centimeter intensity. Such strong illumination can cause significant phototoxicity or even photodamage to fragile biological samples. Therefore, it is highly desirable to find mechanisms that allow the reduction of illumination intensity. Surface plasmon, which is the collective oscillation of electrons in metal under light excitation, is capable of significantly enhancing the local field around the metal nanostructures and thus boosting up the efficiency of nonlinear optical interactions of the surrounding materials or of the metal itself. In this mini-review, we discuss the recent progress of plasmonics in nonlinear optical microscopy with a special focus on biological applications. The advancement of nonlinear imaging modalities (including incoherent/coherent Raman scattering, two/three-photon luminescence, and second/third harmonic generations that have been amalgamated with plasmonics), as well as the novel subdiffraction limit imaging techniques based on nonlinear behaviors of plasmonic scattering, is addressed.

Keywords: metallic nanostructures; cell/tissue imaging; local field enhancement; optical section; near-field microscopy.

1 Introduction

Light-matter interactions have been attracting researchers for ages, as these interactions provide a noninvasive way to probe the material properties and to rapidly detect variations over time. At low intensity, light and matter interact linearly, but the interaction becomes nonlinear at enough high intensity. Although the prediction of nonlinear interactions appeared in the early 20th century [1, 2], various experimental demonstrations, including optical harmonics in scattering, multiphoton absorption, and the saturation of emission, have been boosted up after the invention of lasers in 1960 [3, 4]. These successful experiments led to the rapidly growing research field of nonlinear optics, and a major part focused towards the applications on biology and medicine.

Nowadays, optical nonlinearity is a subject of widespread studies in the photonics community. Nonlinear phenomena provide unique functionalities such as frequency expansion, high harmonic generations, self-focusing, ultra-short pulse control, ultra-fast switching, and all-optical signal processing [5, 6]. However, the optical nonlinearities originate from the material properties of the interacting media and in general are inherently weak. There has been a long quest to improve the efficiency of nonlinear optical processes, and several methods have been proposed/verified, such as by reducing the speed of light [7, 8], by constructing a resonant cavity [9], by quasi-phase matching with periodic structures [10], by elongating the interaction

***Corresponding author: Shi-Wei Chu,** PhD, Department of Physics, National Taiwan University, No. 1, Sec. 4, Roosevelt Road, Taipei 10617, Taiwan, R.O.C; and Molecular Imaging Center, National Taiwan University, No. 1, Sec. 4, Roosevelt Rd, Taipei 10617, Taiwan R.O.C, e-mail: swchu@phys.ntu.edu.tw
Gitanjal Deka: Department of Physics, National Taiwan University, No. 1, Sec. 4, Roosevelt Road, Taipei 10617, Taiwan, R.O.C.
Chi-Kuang Sun: Department of Electrical Engineering, National Taiwan University, No. 1, Sec. 4, Roosevelt Road, Taipei 10617, Taiwan, R.O.C.; and Molecular Imaging Center, National Taiwan University, No. 1, Sec. 4, Roosevelt Road, Taipei 10617, Taiwan, R.O.C.
Katsumasa Fujita: Department of Applied Physics, Osaka University, 2-1 Yamadaoka, Suita, Osaka 565-0851, Japan

Edited by Volker Sorger

length (fiber) [11, 12], by introducing a magnetic field [13, 14], and by local field enhancement [15]. The last effect is related to plasmonics and is the main topic of this review.

Plasmon arises from the collective and coherent oscillation of free electrons in plasma or conduction electrons in metal at optical frequency when excited by light [16, 17]. The field enhancement in general is achieved only in proximity to the plasmonic materials. When the collective oscillation occurs at a surface, such as a metal-dielectric interface, and propagates along the surface, it is called surface plasmon polariton (SPP) [18]. When metals are brought down to nanometer scale, their sizes become comparable to the mean free path of their conduction band electrons (40–50 nm in gold). At this situation, the nanoparticle exhibits intense interaction with incoming light due to localized surface plasmon (LSP) [19, 20]. With appropriate wavelength of incoming light, these localized surface electrons oscillate resonantly, giving rise to the opportunity for controlling light confinement on the nanoscale. The intense electromagnetic interactions associated with these surface plasmon resonance (SPR) nanoparticles depend strongly on the dimension, orientation, and material properties.

SPR on a metallic surface can boost optical nonlinearities in many ways. The coupling of light to SPR can result in extraordinarily strong local electromagnetic fields [17, 21], significantly enhancing optical nonlinear processes of the surrounding materials. Surface-enhanced Raman scattering (SERS) is a prime example of such effect, where SPP excitations at rough or engineered metal surfaces can enhance the inherently weak Raman process by several orders of magnitude, allowing even single-molecule detection [22–24]. Surface plasmon enhancement over thin metallic film can also be used to improve multiphoton fluorescence signals [25]. However, using metal films as the nonlinearity enhancer is typically limited to sample surfaces, so it is very difficult to obtain information from the interior of cells and tissues.

Noble metal nanoparticles, on the contrary, can easily be engulfed by cells or can flow through blood vessels. Evidently, nanoparticle-assisted LSP enhancement of both incoherent and coherent nonlinear processes, including multiphoton fluorescence [26], second harmonic generation (SHG) [27, 28], hyper-Raman scattering [29], and third harmonic generation (THG) [30], have been demonstrated. In a pioneering work, researchers have demonstrated that the presence of gold nanoparticles at cell membranes can simultaneously enhance SHG and quench two-photon fluorescence from nearby dye molecules [28, 31]. Additionally, metallic nanoparticles have less toxicity than quantum dots, making them more biocompatible.

Other than enhancing nonlinear signals from surrounding materials, metal nanostructures are also capable of generating inherent nonlinear optical processes, including SHG [32, 33], multiphoton photoluminescence (PL) [34], THG [35, 36], four-wave mixing (FWM) [37], and excited-state absorption (ESA) [38]. Nanoparticles with different shapes, such as nanorods, exhibit different SPR wavelength bands with varying geometrical parameters and thus allow imaging applications requiring long wavelength for deep penetration. For example, PL from gold nanorods with varying aspect ratios [39] and SHG from plasmonic nanomaterials of various shapes and arrangements have been studied extensively [33, 40–43].

In this mini-review, we discuss the nonlinear processes accompanying plasmonic nanostructures, with an emphasis of imaging applications toward biological cells and tissues either *in vivo* or *in vitro*. In Section 2, we start by briefly reviewing the SPR-enhanced nonlinear processes. In Section 3, nonlinear optical interactions that are enhanced by plasmonics are discussed. In Section 4, inherent nonlinear optical signals from plasmonic nanostructures themselves are reviewed. In Section 5, we describe our recent work about the nonlinear saturation of plasmonic scattering from nanoparticles and the possibilities to enhance far-field imaging resolution. In Section 6, a brief summary and outlook for the future directions is given.

Although nonlinearities of plasmonic nanoparticle have many novel applications in photonics, such as lasing [44], all-optical switching [45, 46], and soliton generation [47, 48], they are not within the scope of this review, whose emphasis is on imaging-related techniques. An excellent review of nonlinear plasmonic can be found in Ref. [49]. In addition, plasmonic nanoparticles are also well known to enhance linear optical processes such as single-photon fluorescence and linear absorption and scattering. In this review, we occasionally mention linear plasmonic interaction in comparison to nonlinear interactions, but the main focus is the latter.

2 Basic principles of nonlinear processes

Nonlinear optical processes arise due to nonlinear interactions of light and matter. As a wide field of research, it contains a broad spectrum of phenomena, such as optical frequency conversion, optical solitons, phase conjugation, and Raman scattering. It is important to note that the linearity of the optical signal with respect to its dependence on incoming light intensity I should not be confused

with the linearity of the light-matter interaction [50]. For example, both single-photon fluorescence and spontaneous Raman emission are linearly related to the incoming light intensity, as shown by Eq. (1):

$$I_{em} \propto I_{ex}, \tag{1}$$

where I_{em} is emission intensity and I_{ex} is excitation intensity. However, the light-matter interaction of the former is linear, whereas spontaneous Raman scattering is a nonlinear interaction between photon (optical field w_1) and phonon (vibrational energy w_v), as shown in Figure 1A, and hence is included in our discussion.

On the contrary, conventional nonlinear optical phenomena are "nonlinear" in the sense that they occur when the response of a material system to an applied optical intensity depends in a nonlinear manner upon the incoming light intensity. When the incoming intensity is low, the molecular dipole oscillates linearly with incoming electric field, creating linear polarization in the material. However, when the incoming intensity is high enough, the dipole oscillation becomes anharmonic, thus creating new radiation frequencies. The nonlinearity can be quantitatively expressed by expansion of the anharmonicity as power series of incident field intensity, as outlined in Eq. (2).

$$I_{em} = \alpha I_{ex}^1 + \beta I_{ex}^2 + \gamma I_{ex}^3 + \ldots\ldots\ldots, \tag{2}$$

where I_{ex} is the applied field intensity and α, β, and γ are linear, second-order nonlinear, and third-order nonlinear coefficients, respectively. It is the linear coefficient that controls the linear optical response, such as absorption, reflection, spontaneous emission, and scattering in a weak field. For strong field intensity, the higher-order coefficients in Eq. (2) need to be considered. Higher-order terms contain components of sums and differences of the incident light frequencies and give rise to radiation at new frequencies, such as SHG and THG.

For second-order nonlinear interactions, SHG, hyper-Rayleigh scattering (HRS), sum, and difference-frequency generation are examples [52]. As shown in Figure 1A, SHG involves the transition of the interacting molecules to a higher-energy virtual state by annihilating two incident photons and generating a new photon at twice frequency of them. Because SHG is only allowed with non-centrosymmetric materials, it provides a structural contrast mechanism for nonlinear microscopy [53].

HRS is a second-order nonlinear phenomenon, similar to SHG, coherently generating new photons with frequency doubled that of incident photons. Nevertheless, unlike SHG, HRS is allowed in isotropic medium dispersed with very small scatterers, and the summation of HRS intensity from scatterers is incoherent [54]. HRS has been extensively used for chemical sensing [55, 56]. Heinz and his group were the first to demonstrate formally that incoherent second-harmonic scattering (i.e. HRS) from spherical plasmonic nanoparticles can be explained based on Mie theory [57].

For third-order nonlinear interactions, we start from FWM. In FWM, three incident photons simultaneously interacting with the material dipole, are annihilated, and generate a new photon whose frequency is a linear combination of the incident photon frequencies. When the frequencies of the incident photons are the same, one of the degenerate processes is called THG, where the energy of the three incident photons adds up together to create an emission photon at tripled frequency, as shown in Figure 1A. Due to the Gouy phase shift, THG is generally

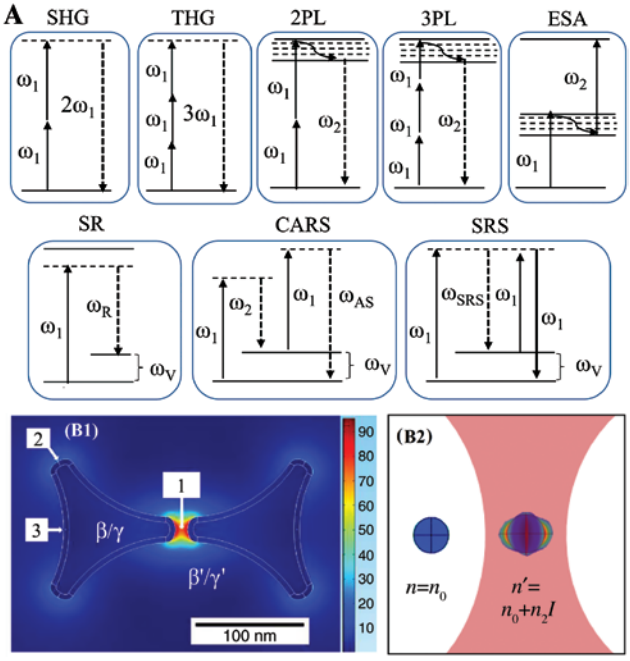

Figure 1: Schematics of electronic transitions in different nonlinear processes and mechanisms of enhancement by plasmonic materials.
(A) The first row: SHG/HRS, THG, 2PL/3PL, ESA the second row: SR (spontaneous Raman), CARS, SRS. (B1) Enhancement of nonlinear effects due to strong localized field of plasmonic structures, with a bowtie nanoantenna as an example. Reprinted with permission from ref. [51]. At the gap of the antenna (position 1), field enhancement is largest, so the nonlinear interaction, as well as the effective nonlinear coefficients (β′, γ′), is also largest. At the antenna tips (position 2), modest field enhancement is present, leading to modest nonlinear signal generation. At position 3, where there is least field enhancement, the nonlinear interaction is weakest (β, γ). (B2) RI variation ($n \rightarrow n'$) of a metal nanoparticle due to plasmon field enhancement when illuminated with a focused laser beam. n_0 is the linear RI of the particle, and n_2 is the nonlinear RI.

observed only at interface or surface, making it a powerful tool for probing physical or chemical properties at the interface [58, 59]. With its third-order power dependency, THG is more confined to the focal point than SHG, so it provides exceptional signal-to-background ratio when applied to an optical section in multiphoton imaging. Furthermore, when the frequencies of the incident photons are not the same, many different FWM configurations exist, and in this review, we mention coherent anti-Stokes Raman scattering (CARS) and stimulated Raman scattering (SRS) [50, 60, 61]. The magnitude of FWM signal strongly depends on the resonance conditions of both incident and induced frequencies. In CARS and SRS, two beams with a frequency difference equal to a vibrational transition energy are used to resonantly and coherently excite the vibration, significantly enhancing the weak Raman interaction and allowing much more rapid detection [50, 62, 63]. In addition, compared to Raman scattering, these coherent Raman techniques provide optical sectioning, as their emission intensity depends nonlinearly with incident intensity. There is another type of nonlinear Raman phenomena called hyper-Raman scattering, in which the emitted frequency is Raman shifted relative to the second harmonic of the incident frequency [29, 54, 64].

As we mentioned earlier, in the 1930s, Dr. Goeppert-Mayer predicted the first nonlinear interaction, which is two-photon absorption. Different from harmonic generations, in two-photon absorption, a molecule transits to a real excited electronic state by simultaneously absorbing two photons. The subsequent luminescence emission due to relaxation is thus called two-photon luminescence (2PL) [65]. Different from harmonic generations, where resonance (real transition) is not necessary, and different from Raman scattering, where the vibrational state is probed, 2PL provides the information of electronic transition structure of the composition materials. On the contrary, similar to harmonic generations, where two- and three-photon interactions exist, there is also three-photon luminescence (3PL), where a molecule is excited by absorbing three photons simultaneously. Similar to THG, 3PL provides better optical sectioning capability due to its high nonlinearity [66, 67].

Other than the simultaneous absorption of multiple photons, another possible nonlinear interaction is to absorb two or three photons sequentially. The process is termed as ESA, in which a pump beam excites molecules into a first excited state and a time-delayed probe beam excites them into a higher excited state by a secondary absorption process. Similar to previous nonlinear processes, ESA provides intrinsic optical sectioning capability [68]. Figure 1 schematically summarizes the second- and third-order nonlinear electronic transitions that we address in this review.

The nonlinear interactions of matter and light can be enhanced by various approaches as mentioned in Section 1. Among them, surface plasmon-enhanced nonlinear processes are relatively simple to implement, and the enhancement efficiency is remarkably high. The enhancement of nonlinear effects in the presence of plasmonic structures may occur in two different ways. First, near the metal-dielectric interface, the energy of photon can be efficiently coupled into either SPPs or LSPs [15], both of which provide significant increased energy density due to the strong confinement. It is the physical mechanism of the field enhancement generally associated with plasmonic resonance. The resulting strong field locally enhances the nonlinear response whether it is the nonlinearity of a material adjacent to the metal (enhanced response) or the inherent nonlinearity of the metal itself (inherent response). The former is the topic of Section 3, and the latter is discussed in Section 4.

Second, the refractive index (RI) of the metal itself or the surrounding dielectric can vary nonlinearly with respect to incident intensity. Because the plasmonic resonance, including both SPP and LSP, are very sensitive to the RI variation, such intensity-dependent RI causes significantly modified plasmonic properties. The corresponding nonlinearity enhancement is described in Section 5. Figure 1B1 and B2 schematically describes the two different nonlinearity enhancement approaches.

3 Plasmonics-enhanced nonlinear processes

The efficiency of nonlinear processes can be increased substantially by plasmonic effect. As mentioned earlier, the coupling of light to coherent oscillation of surface electron of SPP or LSP can result in strong local electromagnetic fields and thus considerably enhance existing nonlinear optical processes. In this section, we focus on nonlinear optical interactions that are already present in the host materials but are relatively weak. These nonlinearities are “enhanced” via the presence of plasmonic nanostructures. Below, we describe the enhancement of various far-field emissions, including multiphoton fluorescence, harmonic generations, Raman scattering, and near-field enhancement with the aid of metallic tips.

3.1 Enhancement of far-field harmonic generations

Surface-enhanced SHG was first detected from rough silver surfaces [69]. From subsequent SHG enhancement experiments on metal-island films and lithographic nanostructures, the role of localized SPR was identified to be the underlying mechanism [70].

Plasmonic nanoparticles, which provide localized field enhancement, are also useful in enhancing harmonic generation signals. Weak SHG from biomolecules have been enhanced by metal nanoparticles [27, 69, 71], leading to widespread applications in biological imaging. For example, metal nanoparticle antibody complexes are directed to specific sites on a cell membrane that has been labeled with a chiral, dipolar, membrane-anchoring dye. Such complexes provide gigantically enhanced nonlinear signals, potentially useful to structural and physiological imaging (Figure 3B) [27, 28]. The same group soon demonstrated functional cellular imaging based on the measurement of membrane potential around a single molecule by plasmonically enhanced SHG from gold nanoparticles [31].

Besides SHG, surface-enhanced THG has also been observed, with a detailed discussion of nanostructure symmetry effects [72]. Yelin et al. have reported not only enhanced THG signals but also two-photon autofluorescence by noble metal nanoparticles attached to cellular organelles and membranes when illuminated by laser in resonance with their plasmon frequency (Figure 3B2 and D1) [26]. We have previously studied the molecular imaging of cancer cells using enhanced THG from silver nanoparticles conjugated with Her2 (Figure 3B1) [73]. Her2 is a transmembrane receptor protein for epidermal growth factors and can be used as predictor for the unfavorable growth behavior of cells. Using nanoparticles as exogenous THG contrast agents, this technique allows us to identify aggressive cancer cells with high molecular specificity. Additionally, we also have demonstrated silver nanoparticle-enhanced THG imaging of collagen fibers and muscle I-band in muscle tissue slices as described in Figure 3C [74].

Other than SHG and THG, the enhancement of FWM, which is a third-order nonlinear optical interaction, by propagating SPPs was demonstrated recently [37]. In that report, it was emphasized on achieving highly directional, coherent, and frequency/angle tunable FWM radiation using local field enhancement at nanostructured surfaces. Their results show the potential for wavelength selection in imaging techniques such as dark-field microscopy. Furthermore, arrays of bowtie antennas were reported to enhance high harmonic generation up to the 17th harmonics and several other nonlinear processes [75, 76]. Basically, the plasmonic nanostructures serve as a nanolens to increase local field strength and can be employed in conjunction with all nonlinear microscopy modalities, including fluorescence and coherent or incoherent Raman scattering, as shown in the following sections.

3.2 Enhancement of far-field multiphoton fluorescence

The first plasmonically enhanced two-photon fluorescence was demonstrated by Kano and Kawata in 1996 [25], where a 90-fold enhancement in total-internal-reflection two-photon fluorescence by SPR was found. As mentioned earlier, plasmonic nanoparticle-enhanced two-photon autofluorescence from cellular organelles was applied to image cells (Figure 3D1) [26]. They are the pioneers who combined SPR field enhancement and nonlinear optical emissions to enhance the contrast of biological imaging. A similar SPR-enhanced two-photon total-internal-reflection fluorescence was recently adopted to image living monkey kidney fibroblast cell membranes transfected with enhanced green fluorescent protein (EGFP; Figure 3D2) [77].

3.3 Enhancement of far-field Raman scattering

Raman scattering is a very useful technique in chemical spectroscopy and label-free imaging applications. The major advantage of Raman scattering is that it provides intrinsic molecular information from vibrational states. However, the main difficulty of incoherent Raman scattering detection is its extremely small cross-section ($\sim 10^{-30}$ cm^{-2}), especially along with the common presence of a strong fluorescence background. Plasmonic nanostructures, with greatly enhanced local field, can introduce substantial signal enhancement for adjacent molecules and make Raman imaging a more practical technique. The enhancement of Raman signal by a plasmonic surface has given rise to a whole new field of research known as SERS [24, 78].

It was first discovered in the 1970s, where 10–14 orders of magnitude higher signal than that of spontaneous Raman spectroscopy was found [79, 80]. Since then, SERS has been extensively used in molecular sensing and imaging both *in vitro* and *in vivo* [19, 23, 81, 82]. SERS is actually sensitive enough to detect even a single biological

molecule without labeling [23, 24, 83]. There are several geometries to obtain active "surfaces" for SERS, such as the surface of a thin metal film [78], patterned surfaces with nanometer-sized roughness [84, 85], metal-coated tip of an atomic force microscopy (AFM) probe [86, 87], or nanoparticles [88–91].

SERS using metal thin surfaces or surfaces with nanometer-sized roughness are useful in sensing biomolecules. Metal-coated AFM probe and solid metal tips are advantageous in SERS imaging with high resolution. However, both flat surfaces and tip probes are used only to image at the surface. On the contrary, nanoparticles have the ability not only to target cell membrane but also to penetrate through it or get endocytose in intracellular vacuoles. SERS has been reportedly used in imaging cells by targeting cell surfaces with Raman-active molecules conjugated with metal nanoparticles [89] and also to detect cancer cell markers, such as Her2, at cell surface [90]. It has also been used in intracellular imaging of live cell cytosol using gold nanoparticle conjugated with SERS reporter [91].

Recently, one of the authors has demonstrated an useful protocol for dynamic SERS imaging equipped with a slit-scanning excitation and nanoparticle-tracking system [81]. Using a single gold nanoparticle engulfed by a vacuole, which travels through the cytosol, this technique allows SERS detection with high spatial and temporal resolution inside a living cell to probe local molecular information. Figure 3E1 shows the electron microscopy image of a macrophage cell with a nanoparticle inside a vacuole. High-speed, high-resolution SERS microspectroscopic imaging with 3D molecular mapping provides insights of organelle transport, membrane protein diffusion, nuclear membrane entry, and rearrangement of cellular cytoskeleton, as shown in Figure 3E2, without chemically or genetically modifying the Raman-active molecules [92, 93].

It is known that the weak scattering efficiency of spontaneous Raman scattering can also be enhanced by coherent excitation based on nonlinear optical interactions, such as hyper-Raman scattering [29], CARS [63, 94], and SRS [95]. By combining SPR field enhancement, the signal intensity of these nonlinear Raman processes can be further improved. For example, Golab et al. have reported an experimental as well as theoretical study of hyper-Raman spectrum of pyridine adsorbed onto roughened silver electrodes. They argued that surface-enhanced hyper-Raman scattering is more sensitive to adsorbate orientation than SERS [29]. Recently, an array of spherical nanocavities in a gold film was used to improve the signal magnitude of CARS spectroscopy by 10^5, and the sensitivity of this surface-enhanced CARS is 1000 times better than SERS [96].

In most examples above, the plasmonic enhancement occurs around metal nanostructures that are either fixed or randomly flowing. It is highly desirable to have a fixed plasmonic structure but with controllable movement. This can be achieved by combining near-field scanning system and a sharp metal tip, as we will discuss in the next section.

3.4 Enhancement by a metallic tip at near field

Scanning probe microscopies such as AFM [97] and near-field scanning optical microscopy (NSOM) [98] have emerged as very useful imaging techniques that provide resolution far beyond the optical diffraction limit. In conventional NSOM, the exceptional high resolution is accomplished by collecting light with a very small aperture in the near-field regime, which is a few tens of nanometers from sample surface. The aperture is typically formed by a tapered fiber tip. However, the tapered design, as well as the shrinked sampling volume, considerably reduces the overall signal strength. An alternative approach is to replace the fiber tip with a metallic tip that can provide efficient coupling between the local field enhancement from the tip and far-field detection [99–101]. The technique is commonly named as tip-enhanced NSOM.

Tip-enhanced NSOM has been applied to almost every optical contrast agents, both linear and nonlinear. In one of the pioneering nonlinear works, Xie's group have demonstrated polarization-dependent tip-enhanced two-photon excited near-field fluorescence imaging using a gold nanotip and a mode-locked Ti:sapphire laser [102]. They imaged photosynthetic membrane fragments from algae with spatial resolutions on the order of 20 nm, as shown in Figure 2F1. Compared to single-photon far-field fluorescence imaging, the combination of near-field and 2PL provides not only greatly enhanced resolution and fluorescence emission but also the reduction of photobleaching. Later on, many other researchers adopted metallic tip-enhanced NSOM for various contrasts, including fluorescence, Raman scattering, and SHG [86, 100, 104–109].

In another pioneering and interesting study, a gold nanoparticle is trapped and controlled by a laser beam to be an imaging probe [110]. By scanning such a trapped gold particle over the sample surface, the enhanced 2PL imaging of fluorescence beads is demonstrated along with single-photon fluorescence imaging of DNA [111]. Nevertheless, although the fluorescence enhancement near a metallic tip or nanoparticle is attractive, it should be noted

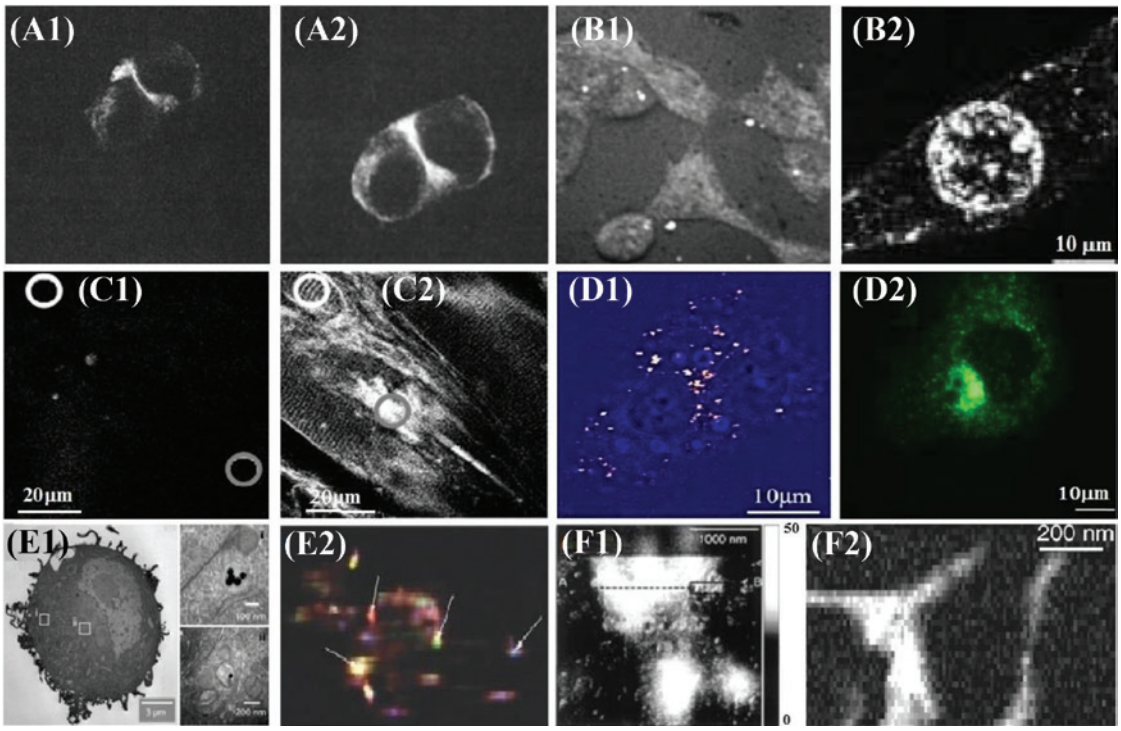

Figure 2: Plasmonics enhanced nonlinear biological imaging.
(A) SHG imaging of neuroblastoma cells (A1) without nanoparticle (A2) enhanced SHG signal after addition of gold nanoparticle. Reprinted with permission from ref [27]. (B1) Silver nanoparticle enhanced THG imaging of wild type MBT2 cells treated with anti-Her2 antibody conjugated Ag nanoparticles. Reprinted with permission from ref [73]. (B2) Plasmon enhanced THG image of a NIH3T3 cell nucleus labelled with 10 nm gold nanoparticles followed by silver enhancement. Reprinted with permission from ref [26]. (C) THG images of a muscle tissue slice (C1) without and (C2) with silver nanoparticle enhanced detection. Gray and white circles indicates the region of THG enhancement from collagen fibers and muscle I-band respectively. Reprinted with permission from ref [74]. (D1) Gold nanoparticle surface plasmon enhanced autofluorescence image (red-yellow) of live Chinese Hamster Ovary cells, superimposed on the transmission image (blue) of the cell. Reprinted with permission from ref [26]. (D2) Surface plasmon-enhanced two-photon total-internal-reflection fluorescence microscopy image of cultured monkey kidney fibroblast cell membrane. Reprinted with permission from ref [77]. (E1) Transmission electron microscope (TEM) observation of macrophages with 50 nm gold nanoparticles, the images in the right display nanoparticles in the vacuole. Reprinted with permission from ref [92]. (E2) SERS images of macrophage cells cultured with 50 nm gold nanoparticles. The white arrows shows regions of high SERS signals. Reprinted with permission from Ref. [93]. (F1) Metal tip excited near field two-photon fluorescence image of photosynthetic membrane fragments of algae (*Chlamydomonas reinhardtii*). Reprinted with permission from ref [102]. (F2) Tip-enhanced CARS image of DNA network. Reprinted with permission from ref [103].

that the requirement of long exposure time in near-field imaging might potentially photobleach the fluorescence.

On the contrary, Raman signal does not suffer from bleach. Raman scattering at near field has attracted a lot of attention with applications toward sensing and imaging. Kawata and his group have done extensive work in plasmon-enhanced near field Raman imaging/detection [112–115]. They have demonstrated that, using aperture-less metal tips, near-field Raman and multiphoton fluorescence imaging of biomolecules can be simultaneously achieved [115]. Later, tip enhancement is further combined with CARS to capture high-resolution images of double-stranded DNA as demonstrated in Figure 2F2 [103]. In an excellent review, various aspects and application of plasmon-enhanced near-field nanoimaging are comprehensively discussed [116].

4 Inherent nonlinear effects of plasmonic nanostructures

Different from what we have described in the previous sections, where plasmonic fields enhance the nonlinearities of adjacent materials, the plasmonic nanostructures themselves also provide inherent nonlinear interactions with light. Such nonlinear behaviors, especially from nanoparticles, can also be used as contrast agencies for optical microscopy in biology.

At this point, we should clarify the difference between inherent and enhanced nonlinear interactions. For example, in Ref. [117], SHG is observed from silver nanoparticles embedded in silica glass. Because silica is a centrosymmetric material, SHG should be forbidden

in the material. Thus, the effect of silver nanoparticles is not to enhance an existing weak SHG source but to generate SHG on their own. As another example, it is known that, due to the Gouy phase shift, THG cancels out in bulk materials and is only observable at interfaces [58]. Therefore, if a metal nanoparticle is placed on a surface, where (weak) THG is allowed, the resulting (strong) THG signal should mostly originate from enhancement [73]. However, if a nanoparticle is immersed in bulk liquid, where THG should be zero, then the emitted THG is more likely to be inherent [35]. In this section, we review the recent progress of various nonlinear optical processes generated inherently by plasmonic nanomaterials and their potential biological imaging applications.

4.1 Inherent harmonic generations

SHG is a nonlinear effect that arises due to light interaction with non-centrosymmetric materials. In the field of microscopy, intrinsic SHG is known to provide structural contrasts in the crystallized biological materials, such as starch granules [118, 119], collagen [27, 120, 121], and skeletal muscles [122, 123]. As discussed in Section 3.1, metallic nanostructures, owing to their SPR, are known to enhance the SHG of the surrounding materials [27, 28, 31, 69]. However, if plasmonic nanostructures break the centrosymmetry by themselves, they exhibit inherent SHG. For example, SHG signal, in transmission mode, from thin layers of ellipsoidal silver nanoparticles embedded in silica glass was detected [117]. Following that, the second harmonic optical response from single silver nanoparticle was reported (Figure 3A1) [124]. Gold nanospheres embedded in dielectric matrix such as gelatin were also reported to generate polarization-dependent SHG signal (Figure 3A2) [32].

The SHG signal strength is highly dependent on the orientation of plasmon oscillation versus excitation light polarization, so SHG can be used as a very sensitive probe to the subtle shape asymmetry of plasmonic nanoparticles [130]. In fact, the SHG dependency of material symmetry and the nanostructure shape open up a series of technique development of *in situ* ultrasensitive nonlinear optical characterization, including the detection of very slight deviations from perfectly symmetric shapes [131, 132] as well as minute surface roughness [133, 134]. Because SHG can point out defects that linear responses cannot, it is attractive in some specific nanoparticle geometries such as the nonlinear optical characterization of gold nanotips by incident beams with azimuthal and radial polarizations [135]. Based on the structural sensitivity, SHG is capable to provide useful information during the chemical synthesis of plasmonic nanoparticles [136–139]. From the same principle but in a completely different context, SHG emission from plasmonic nanoparticles also finds application in laser beam characterization, which is a crucial parameter for laser microscopy and imaging [33, 140].

Regarding biological applications, it has been demonstrated that SHG from plasmonic nanostructures can be used to sensitively detect biological and chemical toxins [56, 141]. In an excellent review, details about the nonlinear optical response from metal nanoparticles and their applications in sensing biomolecules and other chemicals were discussed elaborately [56]. SHG, as well as HRS, from individual plasmonic nanospheres has been used to diagnose single-base-mismatch DNA hybridization [141], to detect Alzheimer's disease biomarkers [142], and to probe heavy metal ions [143]. HRS from gold nanorods are used to selectively detect and identify *Escherichia coli* bacteria [144]. Also, HRS from oval-shaped nanoparticles are used to detect breast cancer cells [145].

There are two remarks for inherent plasmonic SHG as biosensors. The first one is that, although in these literatures no imaging example is provided, these particles are functionalized toward the targeted chemical/biological molecules and are straightforward to molecular imaging applications. The second is that the molecular sensitivity of plasmonic SHG might not be as good as SERS, as illustrated by the comparative studies [146, 147].

Plasmonic nanoparticle have also been reported to exhibit inherent THG signal. THG signals from individual 40 nm gold nanoparticles are first discovered in 2005 (Figure 3B1), enabling the potential for single biomolecule detection and tracking [36]. In that work, a pulsed laser with a center wavelength at 1500 nm is used, so the THG signals peak at 500 nm, matching the plasmonic band of the gold nanoparticles. In 2009, inherent THG from silver nanoparticles, as well as from silicon nanowires, is reported (Figure 3B2) [35]. The authors claimed that THG from silver is less stable than silicon and adopted the later as an imaging contrast for deep-tissue intravital microscopy. However, to the best of our knowledge, inherent plasmonic THG in biological applications is awaiting to be explored.

4.2 Inherent PL emission

Metal nanoparticles are known to have inherent PL [148, 149]. Mooradian was the first to report the experimental detection of single-photon excited PL from noble metals in 1969 [150], where PL was observed as the background

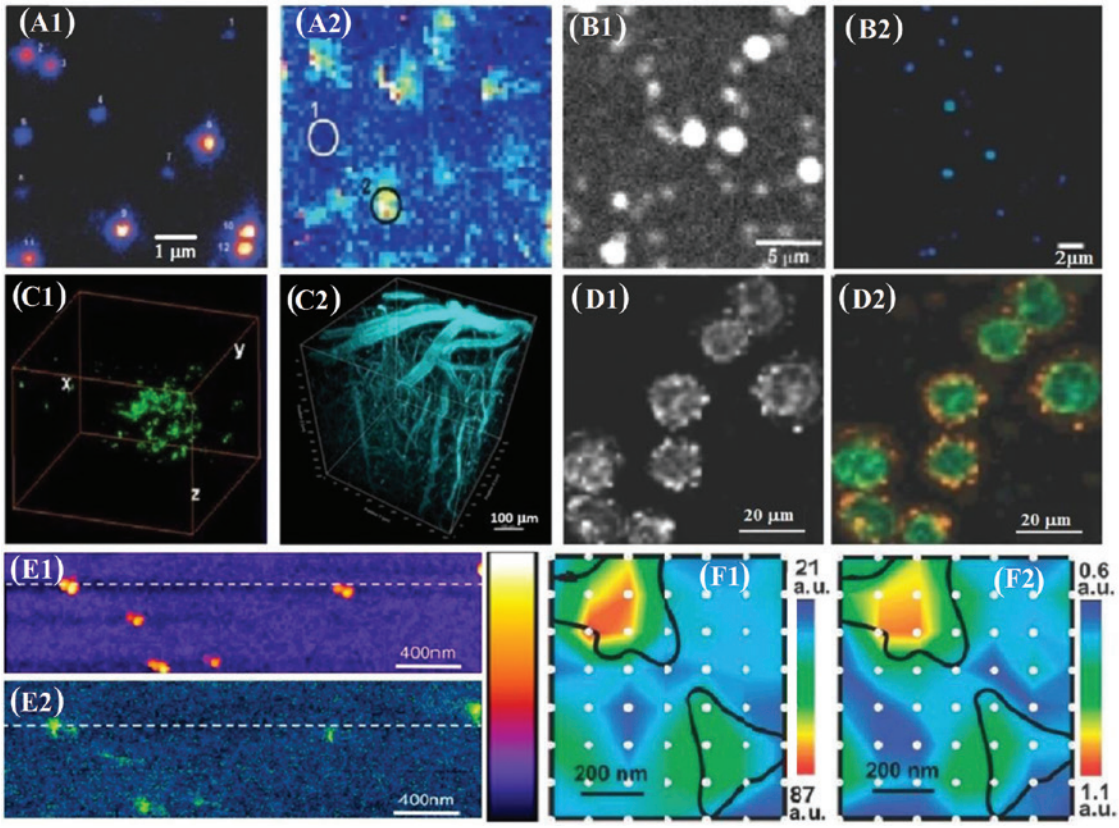

Figure 3: Optical imaging based on inherent nonlinearity of plasmonic nanostructures.
(A) SHG map of individual (A1) silver nanoparticles deposited on a coated substrate. Reprinted with permission from ref [124] and (A2) gold nanoparticles dispersed in gelatin. Reprinted with permission from ref [32]. (B) THG images of (B1) individual gold nanoparticles. Reprinted with permission from ref [36], and (B2) 5 nm silver colloids. Reprinted with permission from ref [35]. The very bright dots in (B1) correspond to 100 nm particles, and the rest are 40 nm particles. (C) Nonlinear PL images in tissues. (C1) Three-dimensional 2PL mapping of gold nanoshells in tumor, with field of view of 124 μm in all three dimensions. Reprinted with permission from ref [125]. (C2) Three-dimensional reconstructed intravital 3PL images of gold nanorod stained mouse brain blood vessels. Reprinted with permission from ref [126]. (D) Two photon microscopy of Karpas-299 cells labeled with gold nanoparticles and H258 dye at the membrane and the nuclear region respectively. The contrasts are based on (D1) intensity, and (D2) fluorescence lifetime. In (D2), the gold nanoparticles (yellow) are clearly distinguishable from the dye (blue-green color) Reprinted with permission from ref [127]. (E) Near-field fluorescence imaging with a gold nano dimer as localized FWM photon source. (E1) Topographic image of monodispersed red fluorescent microspheres. The double-lobed feature is due to the dimer antenna. (E2) Simultaneous near-field fluorescence image. Reprinted with permission from ref [128]. (F) Hyperspectral NSOM mapping the nanotriangles, based on (F1) 2PL and (F2) SHG, respectively. Reprinted with permission from ref [129].

noise in SERS. The luminescence of metal results from several steps of complex interband electronic transitions [148, 150]. Metal nanostructures attract particular interests because of their promising emission properties in terms of outstanding photostability under continuous irradiation, no blinking effects, and the benefit of good biocompatibility. Additionally, metal nanoparticles are advantageous with the ability to tailor the absorption band by modifying the particle geometry (nanospheres, nanoshells, nanorods, nanostars) for specific applications. Both single-photon and multiphoton PL of metal nanoparticles have been shown to correlate strongly with their plasmon resonances [148, 151–153], and they have both been applied to biological imaging.

One interesting example of single-photon PL is to image cancer cells using gold nanoparticles as fluorescent probes engulfed via the endocytic pathways [34]. Due to the exceptional photostability of plasmonic nanoparticles, when the cellular autofluorescence is bleached by strong laser illumination, the nanoparticle PL is unaffected, thus avoiding crosstalk between them.

It is well known that, compared to single-photon confocal techniques, the incorporation of multiphoton imaging techniques provides additional advantages of improved cell viability [154, 155] and deep tissue imaging capabilities [156]. Boyd et al. have first demonstrated enhanced 2PL emission efficiency from a rough metal surface with respect to a flat one [157]. The mechanism of 2PL in the

nanoparticles can be explained by the same electronic transition processes as in surfaces [149]. In general, 2PL is much weaker than single-photon luminescence. However, the weak 2PL signal gets amplified substantially in plasmonic material due to the resonant coupling of the incident light wavelength with localized SPR [25].

In terms of biological applications, plasmonically resonant 2PL from gold nanorods are particularly attractive, because their longitudinal plasmon modes can be tuned to be resonant at near-infrared (NIR), where the absorption of water and most biological molecules is minimized. Wang et al. have reported 60-fold brighter 2PL from gold nanorods than the two-photon fluorescence from a single rhodamine molecule. They have successfully demonstrated the use of 2PL to monitor the flow of individual nanorods through mouse ear blood vessels *in vivo* [149]. They have also argued that nanoparticles with a variety of shapes, including nanosphere, nanorods, nanoshells, and nanocages, can be internalized in macrophages for the *in vivo* monitoring of their dynamics in atherosclerosis and cancer [39, 158].

Recently, sophisticated 2PL correlation spectroscopic detection was adopted to detect gold nanoparticles dispersed in water and flowing through a microfluidic channel that mimics the mammalian blood capillaries [159]. Other than nanorods, 2PL from gold nanoshells is as bright as their nanorods counterparts, also tunable by particle geometry, and has been reported for imaging subcutaneous tumor *in vivo* (Figure 3C1) [125]. Very recently, multimodal gold nanostars for 2PL, SERS, X-ray computed tomography, and photothermal therapy of tumor have been reported. 2PL from the nanostars was used to monitor nanoparticle distribution at the cellular level inside a tumor [160].

To distinguish the 2PL of a metal nanoparticle from cellular autofluorescence, one possible way is to bleach the latter, as we mentioned earlier. An interesting possibility is to adopt luminescence lifetime measurement, because, compared to cellular autofluorescence or dye molecule fluorescence, gold nanoparticles have much shorter PL lifetime. Figure 3D presents the two-photon intensity (Figure 3D1) and fluorescence lifetime (Figure 3D2) images of lymphoma cells labeled with gold nanoparticles (yellow color) and H258 dye (blue-green color) at the membrane and the nuclear region, respectively [127], manifesting their clear distinction in lifetime domain.

With the exceptionally strong resonance nature of SPR, not only 2PL but also 3PL from metal nanoparticles were reported [161, 162]. Bright 3PL from gold and silver alloy nanocage were reported for *in vivo* liver cell imaging with negligible photothermal toxicity and thus excellent cell viability [163]. It is known that higher-order nonlinear signal is better for deep tissue imaging because of not only long excitation wavelength but also the background reduction [67, 164]. Because the three-photon emission of fluorophores is typically weak, plasmonic particles may be an alternative candidate for three-photon deep tissue imaging. The idea is nicely demonstrated in a very recent paper, where 3D reconstructed intravital *in vivo* 3PL imaging of gold nanorod-stained mouse brain blood vessels is presented. High-contrast images are obtained as deep as 600 mm, as shown in Figure 3C2 [126].

Gold nanorods were also reported as probes for selectively imaging live cells with ESA microscopy [38]. Unlike 2PL/3PL microscopy, where contrast comes from luminescence emission, in ESA microscopy, contrast originates from the variation of absorption (loss of transmission). To efficiently decouple weak absorption variation from huge transmission signals, two laser beams along with lock-in detection are generally required for ESA microscopy. The advantage of this relatively complicated set-up is the significantly enhanced sensitivity toward nonfluorescent nanostructures. In the cited work, the location of gold nanorods in cells can be distinguished even under the presence of a strong fluorescence background. Plasmonic nanostructures, including noble metal and graphene, are known to exhibit a large ESA effect or a transient absorption in a more general sense [165, 166]. A noteworthy recent demonstration adopted the saturation of transient absorption in graphene to enhance spatial resolution beyond the diffraction limit without the need of fluorescence [167]. Besides, ESA has been used to image nonplasmonic nanomaterials, such as carbon nanotube and nanodiamond [68]. Although the technique is still in its infancy, it already shows great potential for future biological applications with plasmonic or nonplasmonic nanostructures.

4.3 Near-field imaging by inherent nonlinear emissions

As mentioned in Section 3.4, NSOM is a field where nonlinear plasmonics has extensive applications. Based on the "lightning rod" effect and due to plasmon resonance, immense near fields are generated at the apex of a sharp metal tip, which is able to initiate inherent nonlinear optical process [153]. Here, we focus on inherent nonlinear signals from the NSOM tip. It is found that, when a sharp gold tip is excited with 780 nm femtosecond pulses, nonlinear inherent PL, as well as SHG, is generated [152, 168]. The inherent emission spans across the visible and NIR regions, forming a highly confined white-light continuum

source and exhibiting potential for multispectral imaging for near-field applications.

The same group later expands the concept. They investigated the nonlinear optical properties of gold nanoparticle dimer, which exhibits large field enhancement at its junction [128, 169]. Using two ultrafast lasers at different wavelengths, multiple inherent second- and third-order nonlinearities are induced, including SHG, sum frequency generation, and FWM, significantly expanding the functional wavelength ranges of the plasmonic NSOM. Figure 3E displays the near-field fluorescence imaging of monodispersed red fluorescent particles, of size 40 nm, with this dimer probe technique along with topographic fluorescence image.

Very recently, the inherent linear PL, 2PL, and SHG from gold nanotips are used to achieve background-free nonlinear hyperspectral imaging for gold nanostructures, with resolution down to 30 nm [129]. They have demonstrated a very nice correlation between the tip-sample coupling and sample topography, as shown in Figure 3F1 and F2.

Such tip-generated inherent signals may find applications toward the nonlinear near-field high-resolution imaging of biomolecules. From the above discussion, some of the plasmonic tips have been used in biology, whereas some are not yet. There is still a lot of room left for researchers to explore in this field.

5 Inherent nonlinearity of SPR scattering

In this section, we introduce a very different inherent nonlinearity: saturation and reverse saturation of SPR scattering from a single nanoparticle and its applications toward the resolution enhancement of optical microscopy. The linear scattering of metal nanoparticles, which can be derived from the Mie theory, has been extensively used for biological applications, such as the detection, imaging, or treatment of cancer cells [170–174]. However, the resolutions of these applications, which all belong to far-field optical imaging, are limited by diffraction. Recently, several groundbreaking ideas revolutionized this field with greatly enhanced resolution, which was recognized by the Nobel Prize of Chemistry in 2014. These ideas overcome the diffraction barrier by the switching [175–177] or saturation [178–180] of fluorescence. However, these super resolution techniques are all based on the nonlinear responses of fluorophores under intense laser irradiation, and existing fluorescence molecules quickly bleach under intense laser irradiation. It puts a stringent constraint to fluorophore selections [181, 182] and requests more robust contrast agents [167, 183]. Therefore, it is highly desirable to search for a novel contrast agent that does not bleach.

One of the most appealing candidates is the extraordinarily strong scattering from SPR structures. Nevertheless, the nonlinearity of scattering from a single particle has not been observed until very recently [184, 185]. Our group has demonstrated that scattering signal from even a single gold nanoparticle can be saturated by an intense laser light when the wavelength matches the SPR band of the nanoparticle. The saturated and unsaturated part of the point spread function (PSF) of the nanoparticle can be distinguished to achieve resolution beyond the diffraction limit [186, 187]. The inherent nonlinearity of the gold nanoparticle can be described by the variation of RI with incident intensity:

$$n=n_o+n_2I \tag{3}$$

where n is the total RI, n_o is the linear RI of the particle, and n_2 is nonlinear RI due to field enhancement condition. By assuming that the scattering signal comes from the real part index mismatch D_n between the metallic nanoparticle and the surrounding medium, it is straightforward to express the linear and nonlinear scattering coefficients in terms of linear and nonlinear index mismatch. Apparently, when n_2 is negative, the saturation of scattering occurs.

When the signals saturate, we adopt saturated excitation (SAX) microscopy to enhance the spatial resolution [180]. The principle of SAX microscopy is that, for a laser focal spot, the intensity is stronger at the center than at the periphery. Thus, the saturation should start from the center, whereas the periphery remains unsaturated, as described schematically in Figure 4A. By extracting only the saturated part (i.e. only the central part is left while rejecting the peripheral part), the spatial resolution is effectively enhanced. In SAX implementation, temporal modulation is added onto the excitation source. The scattering signal from the periphery follows the modulation frequency linearly, whereas that from the center does not due to saturation (Figure 4A, right). Transforming the signal into frequency domain, the linear signal in the periphery exhibits only one peak at modulation frequency, but the nonlinear (saturated) signal in the center results in harmonic components. By selectively collecting higher harmonic signals with a lock-in amplifier, and forming an image by scanning the laser beam across the sample, Figure 4B demonstrates resolution enhancement based on scattering from individual gold nanoparticles. Figure 4B1 to B3 corresponds to scattering images constructed by detecting $1f_m$, $2f_m$, and $3f_m$ signals,

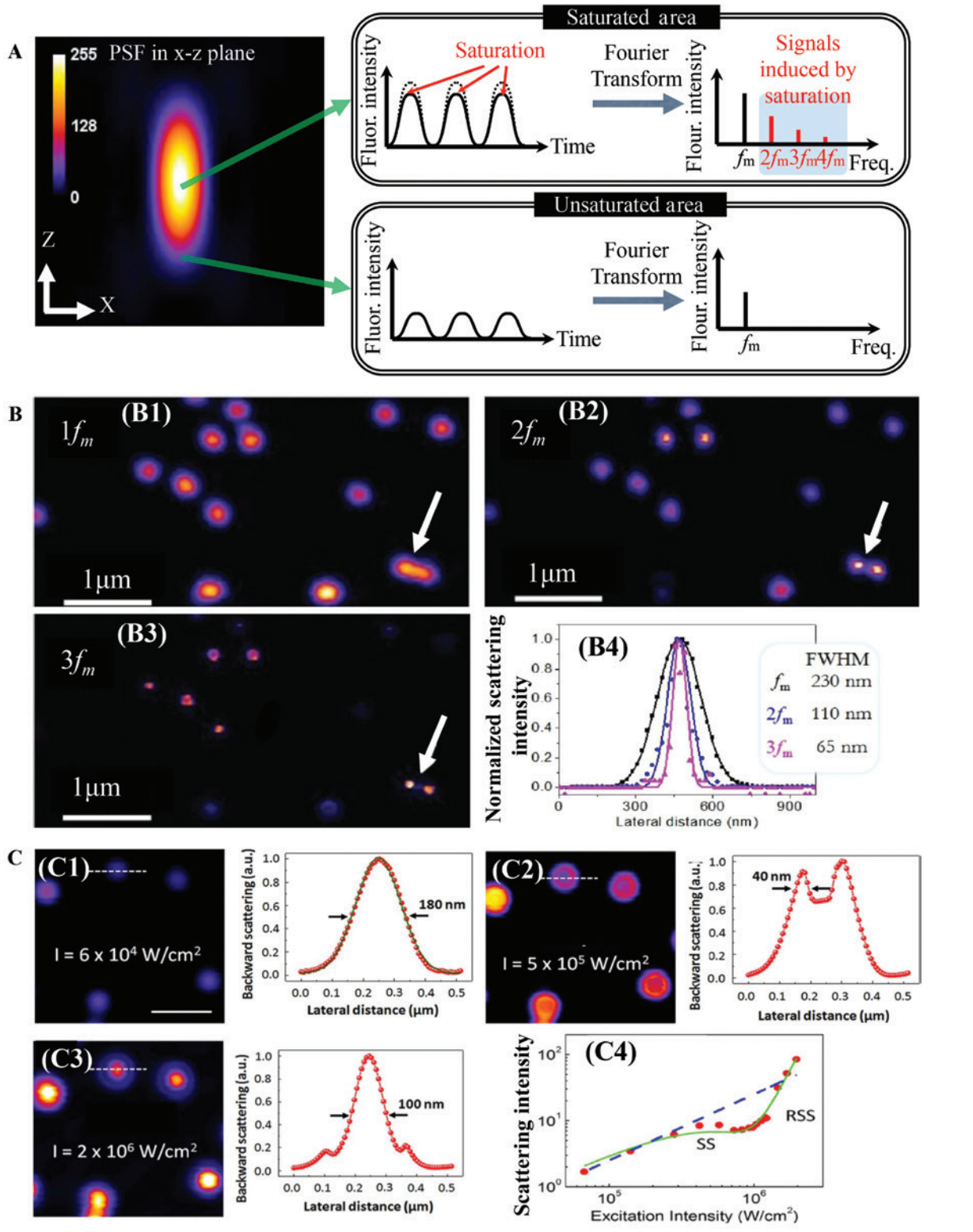

respectively. A white arrow indicates two closely packed nanoparticles that cannot be resolved in Figure 4B1 but can be clearly distinguished with higher harmonic components. The line profiles of single-particle PSFs are given in Figure 4B4, showing a quantitative reduction of full-width at half-maximum (FWHM) to $\lambda/8$, which is much smaller than the diffraction limit.

Without SAX set-up, from the confocal PSFs of well-separated gold nanoparticles with increasing excitation intensity, we find that the inherent nonlinearity of

Figure 4: Nonlinear plasmonic scattering and resolution enhancement with gold nanoparticles.
(A) Left panel is PSF of a single particle scattering in x-z plane, schematically representing saturation at the central region while the periphery is unsaturated. The right panel demonstrates that, with a temporally modulated excitation, higher harmonic components in frequency domain are generated at the central region of the scattering profile, while the scattering signals from the periphery follow the modulation frequency linearly. (B) Resolution enhancement by extracting different modulation harmonic components of the scattering signal. Reprinted with permission from ref [186]. (B1) is taken with fundamental modulation frequency $1f_m$, corresponding to the conventional confocal image. A white arrow indicates two indistinguishable particles. (B2) depicts the image reconstructed from $2f_m$ component of the same scattering signal, where the resolution is improved, and the two particles can be resolved. (B3) depicts the image reconstructed from the $3f_m$ component, and the two nearby nanoparticles are clearly resolved. (B4) The detailed line profiles of a single particle in the scattering images show the resolution enhancement. (C) PSF of scattering from isolated gold nanoparticles with increasing excitation intensity. Reprinted with permission from ref [185]. In (C1–C3), the left panel of each figure shows back-scattering images and the right panel shows the signal profile of a single selected nanoparticle along a white dashed line. (C1) When the excitation intensity is low, the PSF profile fits Gaussian distribution well. (C2) As the intensity increases to 5×10^5 W/cm^2, the scattering signals become saturated, manifested by the valley in the center of the profile. (C3) When the intensity is higher than 10^6 W/cm^2, the scattering signal at the center of PSF increases again, showing the reverse saturated scattering. The FWHM of this PSF is much smaller than the unsaturated one, showing great potential for high-resolution microscopy. Scale bar: 500 nm. (C4) is scattering signal (in red circles) variation against excitation intensity. The green line is a theoretical fitting based on a polynomial equation, and the blue dashed line shows the linear trend.

scattering exhibits not only saturation but also reverse saturation, as shown in Figure 4C. In Figure 4C1, when the excitation intensity is low, a very nice Gaussian profile is observed, manifesting the linear response. In Figure 4C2, at high intensity, saturation occurs, so the scattering intensity at the center part becomes weaker than in the periphery. Very interestingly, in Figure 4C3, at higher intensity, scattering at the center dramatically increases, resulting in a narrow peak with FWHM on the order of 100 nm. The scattering versus excitation intensity dependence is drawn in Figure 4C4, showing complicated nonlinear behavior. Although the nonlinearity can be quantitatively expressed by a polynomial expansion similar to Eq. (2) [187], the underlying mechanism is still under investigation [188]. Because the scattering of nanoparticles has been adopted as a contrast agent for biological imaging, our finding of resolution enhancement based on single-particle scattering paves the way toward subdiffraction limit and long-term observation of biological samples.

6 Conclusion

Nonlinear plasmonics is a young subject and its applications toward bioimaging is still at an early stage. In this mini-review, we have covered the recent progress of plasmonics in nonlinear optical microscopy and their potential biological applications. The intention is to encourage interdisplinary understanding and collaborations. We have addressed the advancement of imaging modalities, including SHG/THG, 2PL/3PL, and incoherent/coherent Raman scattering that are amalgamated with plasmonics, as well as novel subdiffraction limit imaging techniques based on the saturation of plasmonic scattering.

There are two aspects of nonlinear plasmonics, one is the enhancer of nonlinear phenomena within nonplasmonic materials and the other is the inherent nonlinear generator. For the former case, plasmonic field enhancements expedite all the nonlinear processes, allowing the detection of extremely weak nonlinear signals from cell surfaces and interiors. For example, in Section 3.1, two-photon autofluorescence signals from cells and tissues are enhanced by plasmonic particles. On the contrary, based on inherent nonlinearities, plasmonic particles may serve as multipurpose contrast agents. For example, both gold and silver nanoparticles exhibit multiphoton luminescence and SHG/THG. Recently, gold-coated iron nanoparticles are also reported to play dual roles as plasmonic nanoheater and magnetic resonance imaging (MRI) contrasting agent simultaneously [189].

Different geometries of nanostructures have been used for nonlinear plasmonic imaging. Plasmonic metal films were used to enhance nonlinear effects, such as Raman scattering, for molecular sensing. Films are useful for large-scale biological investigation, relatively noninvasive for cells, and relatively easy for sample preparation. Additionally, metal films with arranged nanostructures are reported to provide controllable inherent SHG nonlinear property [27]. However, nonlinear enhancement occurs throughout films, with low spatial selectivity. In addition, the enhancement is limited to sample surface, making it difficult for intracellular imaging.

Using metal tips as scanning probes, significant localized field enhancement at the tip can be achieved. Plasmonic tip-enhanced NSOM provides exceptional high resolution down to a few nanometers and is a rapidly growing field in biological imaging. However, near-field phenomena are also restricted to topographic imaging at

the surface, and the speed is typically much slower than cellular dynamics. At present, active researches in this field focus on several directions such as optimizing the optical antenna probe in terms of size, gain, directivity, ease of fabrication, reproducibility, etc., and at the same time increasing the pool of probe options. Within our review, we mentioned that several inherent nonlinear processes from plasmonic tips exhibit potential but are yet to be used in high-resolution biological applications. In the future, the unison of plasmonic effect with other scanning probe as well as time-resolved optical techniques will further advance tip-enhanced NSOM with respect to a wide range of applicability, signal enhancement, and spatial resolution.

Compared to films and tips, metal nanoparticles provide a unique advantage of imaging deeper than surface in a cell or tissue. Because of their small dimensions that allow endocytosis, metal nanoparticles are applicable for intracellular or even *in vivo* observation. The PL emission efficiency of plasmonic nanoparticles is much larger compared to fluorescent molecules, and their toxicity towards cells is much less compared to quantum dots. Hence, nanoparticles can fill the niche of contrast agent between fluorophores and quantum dots. On the contrary, nanoparticles also exhibit their own limitations. Similar to all external labeling, using nanoparticles as contrast agents may interfere with cellular or molecular functions. Compared to fluorescence molecules, nanoparticles are relatively large, so the interference might be stronger. Additionally, during the chemical fabrication of nanoparticles, it is difficult to maintain the size/shape uniformity, leading to varying resonance conditions, which in turn results in inefficient signal enhancement.

Different from PL, only virtual transitions are involved during harmonic generation processes, so the potential heat generation is less and the signal is more stable. One of the future directions is higher harmonic generation signal from gold and silver nanoparticles, which are waiting to be incorporated into the biological imaging domain. As a three-photon phenomenon, plasmonic THG has a huge potential for deep tissue *in vivo* imaging with minimum background. The tunability of plasmonic band by varying the sizes and shapes of nanoparticles provides a wide spectrum of application possibilities with both luminescence and harmonic generation modalities.

In this review, we have mentioned many different plasmonic nanostructures that have been applied in biology, whereas some are yet to be explored. In terms of materials, although we mainly discussed gold and silver nanostructures as the plasmonic filed enhancer, there are several other potential candidates as evaluated in an excellent review [190], such as platinum [191], copper [192], aluminum [193], gold- and silver-coated iron [189, 194], and graphene, which recently has also emerged as a promising candidate due to its unique electronic properties [195]. On the contrary, some nonlinear optical interactions, such as sum frequency generation, which is very useful to probe non-centrosymmetric structures or molecular vibrational states [196], have not been combined with plasmonics for imaging. In the future, there are still plenty of opportunities to play with nonlinear plasmonic effects and their applications in biology.

Acknowledgments: This study was supported by the National Science Council grants NSC-101-2923-M-002-001-MY3 and NSC 102-2112-M-002-018-MY3. This research was also supported by the Japan Society for the Promotion of Science (JSPS) through the "Funding Program for Next Generation World-Leading Researchers (NEXT Program)", initiated by the Council for Science and Technology Policy (CSTP) and JSPS Asian CORE Program.

References

[1] Göppert-Mayer M. Über elementarakte mit zwei quantensprüngen. Ann Phys-Berl 1931;401:273–94.
[2] Raman CV, Krishnan KS. A new type of secondary radiation. Nature 1928;121:501–2.
[3] Franken PA, Hill AE, Peters CW, Weinreich G. Generation of optical harmonics. Phys Rev Lett 1961;7:118–9.
[4] Maiman TH. Stimulated optical radiation in ruby. Nature 1960;187:493–4.
[5] Boyd RW. Nonlinear optics. San Diego, CA: Academic Press, 2002.
[6] Shen YR. The principles of nonlinear optics. Hoboken, NJ: John Wiley & Sons, Inc., 2003.
[7] Heebner JE, Boyd RW, Park Q-H. Slow light, induced dispersion, enhanced nonlinearity, and optical solitons in a resonator-array waveguide. Phys Rev E 2002;65:036619.
[8] Monat C, De Sterke M, Eggleton B. Slow light enhanced nonlinear optics in periodic structures. J Opt 2010;12:104003.
[9] Melloni A, Morichetti F, Martinelli M. Linear and nonlinear pulse propagation in coupled resonator slow-wave optical structures. Opt Quant Electron 2003;35:365–79.
[10] Fejer MM, Magel G, Jundt DH, Byer RL. Quasi-phase-matched second harmonic generation: tuning and tolerances. IEEE J Quant Elect 1992;28:2631–54.
[11] Foster MA, Turner AC, Lipson M, Gaeta AL. Nonlinear optics in photonic nanowires. Opt Express 2008;16:1300–20.
[12] Russell PS, Holzer P, Chang W, Abdolvand A, Travers JC. Hollow-core photonic crystal fibres for gas-based nonlinear optics. Nat Photon 2014;8:278–86.
[13] Pustogowa U, Hübner W, Bennemann K. Enhancement of the magneto-optical Kerr angle in nonlinear optical response. Phys Rev B 1994;49:10031.
[14] Klein MW, Wegener M, Feth N, Linden S. Experiments on second- and third-harmonic generation from magnetic metamaterials. Opt Express 2007;15:5238–47.

[15] Maier SA. Plasmonics: fundamentals and applications. Bath, United Kingdom: Springer Science & Business Media, 2007.
[16] Stockman MI. Nanoplasmonics: past, present, and glimpse into future. Opt Express 2011;19:22029–106.
[17] Zayats AV, Smolyaninov II, Maradudin AA. Nano-optics of surface plasmon polaritons. Phys Rep 2005;408:131–4.
[18] Pitarke J, Silkin V, Chulkov E, Echenique P. Theory of surface plasmons and surface-plasmon polaritons. Rep Prog Phys 2007;70:1.
[19] Willets KA, Van Duyne RP. Localized surface plasmon resonance spectroscopy and sensing. Annu Rev Phys Chem 2007;58: 267–97.
[20] Hutter E, Fendler JH. Exploitation of localized surface plasmon resonance. Adv Mater 2004;16:1685–706.
[21] Novotny L, Van Hulst N. Antennas for light. Nat Photon 2011;5:83–90.
[22] Sharma S, Frontiera RR, Henry A-I, Ringe E, Van Duyne RP. SERS: materials, applications, and the future. Mater Today 2012;15:16–25.
[23] Nie S, Emory SR. Probing single molecules and single nanoparticles by surface-enhanced Raman scattering. Science 1997;275:1102–6.
[24] Kneipp K, Wang Y, Kneipp H, Perelman LT, Itzkan I, Dasari RR, Feld MS. Single molecule detection using surface-enhanced Raman scattering (SERS). Phys Rev Lett 1997;78:1667.
[25] Kano H, Kawata S. Two-photon-excited fluorescence enhanced by a surface plasmon. Opt Lett 1996;21:1848–50.
[26] Yelin D, Oron D, Thiberge S, Moses E, Silberberg Y. Multiphoton plasmon-resonance microscopy. Opt Express 2003;11:1385–91.
[27] Campagnola PJ, Clark HA, Mohler WA, Lewis A, Loew LM. Second-harmonic imaging microscopy of living cells. J Biomed Opt 2001;6:277–86.
[28] Peleg G, Lewis A, Bouevitch O, Loew L, Parnas D, Linial M. Gigantic optical non-linearities from nanoparticle-enhanced molecular probes with potential for selectively imaging the structure and physiology of nanometric regions in cellular systems. Bioimaging 1996;4:215–24.
[29] Golab J, Sprague J, Carron K, Schatz G, Van Duyne R. A surface enhanced hyper-Raman scattering study of pyridine adsorbed onto silver: experiment and theory. J Chem Phys 1988;88:7942–51.
[30] Tsang TY. Surface-plasmon-enhanced third-harmonic generation in thin silver films. Opt Lett 1996;21:245–7.
[31] Peleg G, Lewis A, Linial M, Loew LM. Nonlinear optical measurement of membrane potential around single molecules at selected cellular sites. Proc Natl Acad Sci USA 1999;96:6700–4.
[32] Butet J, Duboisset J, Bachelier G, Russier-Antoine I, Benichou E, Jonin C, Brevet P-F. Optical second harmonic generation of single metallic nanoparticles embedded in a homogeneous medium. Nano Lett 2010;10:1717–21.
[33] Butet J, Brevet P-F, Martin OJF. Optical second harmonic generation in plasmonic nanostructures: from fundamental principles to advanced applications. ACS Nano 2015;9:10545–62.
[34] He H, Xie C, Ren J. Nonbleaching fluorescence of gold nanoparticles and its applications in cancer cell imaging. Anal Chem 2008;80:5951–7.
[35] Jung Y, Tong L, Tanaudommongkon A, Cheng J-X, Yang C. *In vitro* and *in vivo* nonlinear optical imaging of silicon nanowires. Nano Lett 2009;9:2440–4.
[36] Lippitz M, van Dijk MA, Orrit M. Third-harmonic generation from single gold nanoparticles. Nano Lett 2005;5:799–802.
[37] Renger J, Quidant R, Van Hulst N, Novotny L. Surface-enhanced nonlinear four-wave mixing. Phys Rev Lett 2010;104:046803.
[38] Chen T, Chen S, Zhou J, Liang D, Chen X, Huang Y. Transient absorption microscopy of gold nanorods as spectrally orthogonal labels in live cells. Nanoscale 2014;6:10536–9.
[39] Wang T, Halaney D, Ho D, Feldman MD, Milner TE. Two-photon luminescence properties of gold nanorods. Biomed Opt Express 2013;4:584–95.
[40] Singh AK, Senapati D, Neely A, Kolawole G, Hawker C, Ray PC. Nonlinear optical properties of triangular silver nanomaterials. Chem Phys Lett 2009;481:94–8.
[41] Zhang Y, Grady NK, Ayala-Orozco C, Halas NJ. Three-dimensional nanostructures as highly efficient generators of second harmonic light. Nano Lett 2011;11:5519–23.
[42] Linden S, Niesler F, Förstner J, Grynko Y, Meier T, Wegener M. Collective effects in second-harmonic generation from split-ring-resonator arrays. Phys Rev Lett 2012;109:015502.
[43] Valev V, Smisdom N, Silhanek A, De Clercq B, Gillijns W, Ameloot M, Moshchalkov V, Verbiest T. Plasmonic ratchet wheels: switching circular dichroism by arranging chiral nanostructures. Nano Lett 2009;9:3945–8.
[44] Berini P, De Leon I. Surface plasmon-polariton amplifiers and lasers. Nat Photon 2012;6:16–24.
[45] Min C, Wang P, Chen C, Deng Y, Lu Y, Ming H, Ning T, Zhou Y, Yang G. All-optical switching in subwavelength metallic grating structure containing nonlinear optical materials. Opt Lett 2008;33:869–71.
[46] Ren M, Jia B, Ou JY, Plum E, Zhang J, MacDonald KF, Nikolaenko AE, Xu J, Gu M, Zheludev NI. Nanostructured plasmonic medium for terahertz bandwidth all-optical switching. Adv Mater 2011;23:5540–4.
[47] Davoyan AR, Shadrivov IV, Kivshar YS. Self-focusing and spatial plasmon-polariton solitons. Opt Express 2009;17:21732–7.
[48] Liu Y, Bartal G, Genov DA, Zhang X. Subwavelength discrete solitons in nonlinear metamaterials. Phys Rev Lett 2007;99:153901.
[49] Kauranen M, Zayats AV. Nonlinear plasmonics. Nat Photon 2012;6:737–48.
[50] Cheng J-X, Xie XS. Coherent Raman scattering microscopy. New York: CRC Press, 2012.
[51] Herr U, Kuerbanjiang B, Benel C, Papageorgiou G, Goncalves M, Boneberg J, Leiderer P, Ziemann P, Marek P, Hahn H. Near-field effects and energy transfer in hybrid metal-oxide nanostructures. Beilstein J Nanotechnol 2013;4:306–17.
[52] Yue S, Slipchenko MN, Cheng J-X. Multimodal nonlinear optical microscopy. Laser Photon Rev 2011;5:496–512.
[53] Gannaway J, Sheppard C. Second-harmonic imaging in the scanning optical microscope. Opt Quant Electron 1978;10:435–9.
[54] Roke S, Gonella G. Nonlinear light scattering and spectroscopy of particles and droplets in liquids. Annu Rev Phys Chem 2012;63:353–78.
[55] Clays K, Persoons A. Hyper-Rayleigh scattering in solution. Phys Rev Lett 1991;66:2980–3.
[56] Ray PC. Size and shape dependent second order nonlinear optical properties of nanomaterials and their application in biological and chemical sensing. Chem Rev 2010;110:5332–65.

[57] Dadap JI, Shan J, Eisenthal KB, Heinz TF. Second-harmonic Rayleigh scattering from a sphere of centrosymmetric material. Phys Rev Lett 1999;83:4045.
[58] Cheng J-X, Xie XS. Green's function formulation for third-harmonic generation microscopy. J Opt Soc Am B 2002;19:1604–10.
[59] Sun C-K, Chu S-W, Tai S-P, Keller S, Mishra UK, DenBaars SP. Scanning second-harmonic/third-harmonic generation microscopy of gallium nitride. Appl Phys Lett 2000;77:2331–3.
[60] Huang L, Cheng J-X. Nonlinear optical microscopy of single nanostructures. Annu Rev Mater Res 2013;43:213–36.
[61] Mukamel S. Principles of nonlinear optical spectroscopy. Rochester, NY: Oxford University Press, 1999.
[62] Min W, Freudiger CW, Lu S, Xie XS. Coherent nonlinear optical imaging: beyond fluorescence microscopy. Annu Rev Phys Chem 2011;62:507–30.
[63] Zumbusch A, Holtom GR, Xie XS. Three-dimensional vibrational imaging by coherent anti-Stokes Raman scattering. Phys Rev Lett 1999;82:4142–5.
[64] Terhune R, Maker P, Savage C. Measurements of nonlinear light scattering. Phys Rev Lett 1965;14:681–4.
[65] Lakowicz JR. Principles of fluorescence spectroscopy. New York: Plenum Press, 1999.
[66] Hell SW, Bahlmann K, Schrader M, Soini A, Malak HM, Gryczynski I, Lakowicz JR. Three-photon excitation in fluorescence microscopy. J Biomed Opt 1996;1:71–4.
[67] Horton NG, Wang K, Kobat D, Clark CG, Wise FW, Schaffer CB, Xu C. In vivo three-photon microscopy of subcortical structures within an intact mouse brain. Nat Photon 2013;7:205–9.
[68] Chen T, Huang Y. Transient absorption: a new modality for microscopic imaging of nanomaterials in living cells. Small 2015;11:4998–5003.
[69] Chen C, De Castro A, Shen Y. Surface-enhanced second-harmonic generation. Phys Rev Lett 1981;46:145–8.
[70] Wokaun A, Bergman J, Heritage J, Glass A, Liao P, Olson D. Surface second-harmonic generation from metal island films and microlithographic structures. Phys Rev B 1981;24:849–56.
[71] Chen B, Estrada LC, Hellriegel C, Gratton E. Nanometer-scale optical imaging of collagen fibers using gold nanoparticles. Biomed Opt Express 2011;2:511–9.
[72] Kim E, Elovikov S, Murzina T, Nikulin A, Aktsipetrov O, Bader M, Marowsky G. Surface-enhanced optical third-harmonic generation in Ag island films. Phys Rev Lett 2005;95:227402.
[73] Tai S-P, Wu Y, Shieh D-B, Chen L-J, Lin K-J, Yu C-H, Chu S-W, Chang C-H, Shi X-Y, Wen Y-C. Molecular imaging of cancer cells using plasmon-resonant-enhanced third-harmonic-generation in silver nanoparticles. Adv Mater 2007;19:4520–3.
[74] Chu SW, Chen SY, Chern GW, Tsai TH, Chen YC, Lin BL, Sun CK. Studies of c(2)/c(3) tensors in submicron-scaled bio-tissues by polarization harmonics optical microscopy. Biophys J 2004;86:3914–22.
[75] Kim S, Jin J, Kim Y-J, Park I-Y, Kim Y, Kim S-W. High-harmonic generation by resonant plasmon field enhancement. Nature 2008;453:757–60.
[76] Ko KD, Kumar A, Fung KH, Ambekar R, Liu GL, Fang NX, Toussaint KC Jr. Nonlinear optical response from arrays of Au bowtie nanoantennas. Nano Lett 2010;11:61–5.
[77] He R-Y, Su Y-D, Cho K-C, Lin C-Y, Chang N-S, Chang C-H, Chen S-J. Surface plasmon-enhanced two-photon fluorescence microscopy for live cell membrane imaging. Opt Express 2009;17:5987–97.
[78] Campion A, Kambhampati P. Surface-enhanced Raman scattering. Chem Soc Rev 1998;27:241–50.
[79] Fleischmann M, Hendra PJ, McQuillan A. Raman spectra of pyridine adsorbed at a silver electrode. Chem Phys Lett 1974;26:163–6.
[80] McQuillan AJ. The discovery of surface-enhanced Raman scattering. Notes Rec R Soc 2009;63:105–9.
[81] Palonpon AF, Ando J, Yamakoshi H, Dodo K, Sodeoka M, Kawata S, Fujita K. Raman and SERS microscopy for molecular imaging of live cells. Nat Photon 2013;8:677–92.
[82] Beermann J, Novikov SM, Leosson K, Bozhevolnyi SI. Surface enhanced Raman microscopy with metal nanoparticle arrays. J Opt A Pure Appl Opt 2009;11:075004.
[83] Michaels AM, Nirmal M, Brus L. Surface enhanced Raman spectroscopy of individual rhodamine 6G molecules on large Ag nanocrystals. J Am Chem Soc 1999;121:9932–9.
[84] Hennigan SL, Driskell JD, Dluhy RA, Zhao Y, Tripp RA, Waites KB, Krause DC. Detection of *Mycoplasma pneumoniae* in simulated and true clinical throat swab specimens by nanorod array-surface-enhanced Raman spectroscopy. PLoS One 2010;5:e13633.
[85] Freeman RG, Grabar KC, Allison KJ, Bright RM. Self-assembled metal colloid monolayers: an approach to SERS substrates. Science 1995;267:1629.
[86] Bailo E, Deckert V. Tip-enhanced Raman scattering. Chem Soc Rev 2008;37:921–30.
[87] Anderson MS. Locally enhanced Raman spectroscopy with an atomic force microscope. Appl Phys Lett 2000;76:3130–2.
[88] Zeiri L, Bronk B, Shabtai Y, Eichler J, Efrima S. Surface-enhanced Raman spectroscopy as a tool for probing specific biochemical components in bacteria. Appl Spectrosc 2004;58:33–40.
[89] Hu Q, Tay L-L, Noestheden M, Pezacki JP. Mammalian cell surface imaging with nitrile-functionalized nanoprobes: biophysical characterization of aggregation and polarization anisotropy in SERS imaging. J Am Chem Soc 2007;129:14–5.
[90] KyuáLee E, YoungáShin S, HanáLee Y, WookáSon S, HwanáOh C, MyongáSong J, HoáKang S. SERS imaging of HER2-overexpressed MCF7 cells using antibody-conjugated gold nanorods. Phys Chem Chem Phys 2009;11:7444–9.
[91] Kneipp J, Kneipp H, Rajadurai A, Redmond RW, Kneipp K. Optical probing and imaging of live cells using SERS labels. J Raman Spectrosc 2009;40:1–5.
[92] Ando J, Fujita K, Smith NI, Kawata S. Dynamic SERS imaging of cellular transport pathways with endocytosed gold nanoparticles. Nano Lett 2011;11:5344–8.
[93] Ando J, Yano T-A, Fujita K, Kawata S. Metal nanoparticles for nano-imaging and nano-analysis. Phys Chem Chem Phys 2013;15:13713–22.
[94] Duncan MD, Reintjes J, Manuccia T. Scanning coherent anti-Stokes Raman microscope. Opt Lett 1982;7:350–2.
[95] Freudiger CW, Min W, Saar BG, Lu S, Holtom GR, He C, Tsai JC, Kang JX, Xie XS. Label-free biomedical imaging with high sensitivity by stimulated Raman scattering microscopy. Science 2008;322:1857–61.
[96] Steuwe C, Kaminski CF, Baumberg JJ, Mahajan S. Surface enhanced coherent anti-Stokes Raman scattering on nanostructured gold surfaces. Nano Lett 2011;11:5339–43.
[97] Binnig G, Gerber C, Stoll E, Albrecht T, Quate C. Atomic resolution with atomic force microscope. Europhys Lett 1987;3:1281.

[98] Dunn RC. Near-field scanning optical microscopy. Chem Rev 1999;99:2891–928.
[99] Bouhelier A, Renger J, Beversluis MR, Novotny L. Plasmon-coupled tip-enhanced near-field optical microscopy. J Microsc 2003;210:220–4.
[100] Huang FM, Festy F, Richards D. Tip-enhanced fluorescence imaging of quantum dots. Appl Phys Lett 2005;87:183101.
[101] Mauser N, Hartschuh A. Tip-enhanced near-field optical microscopy. Chem Soc Rev 2014;43:1248–62.
[102] Sánchez EJ, Novotny L, Xie XS. Near-field fluorescence microscopy based on two-photon excitation with metal tips. Phys Rev Lett 1999;82:4014–7.
[103] Ichimura T, Hayazawa N, Hashimoto M, Inouye Y, Kawata S. Tip-enhanced coherent anti-Stokes Raman scattering for vibrational nanoimaging. Phys Rev Lett 2004;92:220801.
[104] Lakowicz JR, Geddes CD, Gryczynski I, Malicka JB, Gryczynski Z, Aslan K, Lukomska J, Huang J. Advances in surface-enhanced fluorescence. In Biomed Opt. International Society for Optics and Photonics, 2004, pp. 10–28.
[105] Bharadwaj P, Anger P, Novotny L. Nanoplasmonic enhancement of single-molecule fluorescence. Nanotechnology 2007;18:044017.
[106] Gerton JM, Wade LA, Lessard GA, Ma Z, Quake SR. Tip-enhanced fluorescence microscopy at 10 nanometer resolution. Phys Rev Lett 2004;93:180801.
[107] Vinegoni C, Ralston T, Tan W, Luo W, Marks DL, Boppart SA. Integrated structural and functional optical imaging combining spectral-domain optical coherence and multiphoton microscopy. Appl Phys Lett 2006;88:053901.
[108] Steidtner J, Pettinger B. Tip-enhanced Raman spectroscopy and microscopy on single dye molecules with 15 nm resolution. Phys Rev Lett 2008;100:236101.
[109] Zayats AV, Sandoghdar V. Apertureless scanning near-field second-harmonic microscopy. Opt Commun 2000;178:245–9.
[110] Sugiura T, Okada T, Inouye Y, Nakamura O, Kawata S. Gold-bead scanning near-field optical microscope with laser-force position control. Opt Lett 1997;22:1663–5.
[111] Sugiura T, Okada T. Near-field scanning optical microscope with an optically trapped metallic Rayleigh particle. In BiOS'98 International Biomedical Optics Symposium. International Society for Optics and Photonics, 1998, pp. 4–14.
[112] Inouye Y, Kawata S. Near-field scanning optical microscope with a metallic probe tip. Opt Lett 1994;19:159–61.
[113] Hayazawa N, Inouye Y, Sekkat Z, Kawata S. Near-field Raman scattering enhanced by a metallized tip. Chem Phys Lett 2001;335:369–74.
[114] Furukawa H, Kawata S. Local field enhancement with an apertureless near-field-microscope probe. Opt Commun 1998;148:221–4.
[115] Hayazawa N, Inouye Y, Sekkat Z, Kawata S. Metallized tip amplification of near-field Raman scattering. Opt Commun 2000;183:333–6.
[116] Kawata S, Inouye Y, Verma P. Plasmonics for near-field nano-imaging and superlensing. Nat Photon 2009;3:388–94.
[117] Podlipensky A, Lange J, Seifert G, Graener H, Cravetchi I. Second-harmonic generation from ellipsoidal silver nanoparticles embedded in silica glass. Opt Lett 2003;28:716–8.
[118] Mizutani G, Sonoda Y, Sano H, Sakamoto M, Takahashi T, Ushioda S. Detection of starch granules in a living plant by optical second harmonic microscopy. J Lumin 2000;87:824–6.
[119] Zhuo Z-Y, Liao C-S, Huang C-H, Yu J-Y, Tzeng Y-Y, Lo W, Dong C-Y, Chui H-C, Huang Y-C, Lai H-M. Second harmonic generation imaging – a new method for unraveling molecular information of starch. J Struct Biol 2010;171:88–94.
[120] Chu S-W, Chen S-Y, Chern G-W, Tsai T-H, Chen Y-C, Lin B-L, Sun C-K. Studies of $\chi^{(2)}/\chi^{(3)}$ tensors in submicron-scaled bio-tissues by polarization harmonics optical microscopy. Biophys J 2004;86:3914–22.
[121] Chu SW, Tai SP, Chan MC, Sun CK, Hsiao IC, Lin CH, Chen YC, Lin BL. Thickness dependence of optical second harmonic generation in collagen fibrils. Opt Express 2007;15:12005–10.
[122] Plotnikov SV, Millard AC, Campagnola PJ, Mohler WA. Characterization of the myosin-based source for second-harmonic generation from muscle sarcomeres. Biophys J 2006;90:693–703.
[123] Chu SW, Tai SP, Liu TM, Sun CK, Lin CH. Selective imaging in second-harmonic-generation microscopy with anisotropic radiation. J Biomed Opt 2009;14:010504.
[124] Jin R, Jureller JE, Kim HY, Scherer NF. Correlating second harmonic optical responses of single Ag nanoparticles with morphology. J Am Chem Soc 2005;127:12482–3.
[125] Park J, Estrada A, Sharp K, Sang K, Schwartz JA, Smith DK, Coleman C, Payne JD, Korgel BA, Dunn AK. Two-photon-induced photoluminescence imaging of tumors using near-infrared excited gold nanoshells. Opt Express 2008;16:1590–9.
[126] Wang S, Xi W, Cai F, Zhao X, Xu Z, Qian J, He S. Three-photon luminescence of gold nanorods and its applications for high contrast tissue and deep *in vivo* brain imaging. Theranostics 2015;5:251–66.
[127] Qu X, Wang J, Zhang Z, Koop N, Rahmanzadeh R, Hüttmann G. Imaging of cancer cells by multiphoton microscopy using gold nanoparticles and fluorescent dyes. J Biomed Opt 2008;13:031217.
[128] Palomba S, Danckwerts M, Novotny L. Nonlinear plasmonics with gold nanoparticle antennas. J Opt A Pure Appl Opt 2009;11:114030.
[129] Horneber A, Braun K, Rogalski J, Leiderer P, Meixner AJ, Zhang D. Nonlinear optical imaging of single plasmonic nanoparticles with 30 nm resolution. Phys Chem Chem Phys 2015;17:21288–93.
[130] Czaplicki R, Mäkitalo J, Siikanen R, Husu H, Lehtolahti J, Kuittinen M, Kauranen M. Second-harmonic generation from metal nanoparticles: resonance enhancement versus particle geometry. Nano Lett 2014;15:530–4.
[131] Nappa J, Revillod G, Russier-Antoine I, Benichou E, Jonin C, Brevet P. Electric dipole origin of the second harmonic generation of small metallic particles. Phys Rev B 2005;71:165407.
[132] Bachelier G, Russier-Antoine I, Benichou E, Jonin C, Brevet P-F. Multipolar second-harmonic generation in noble metal nanoparticles. J Opt Soc Am B 2008;25:955–60.
[133] O'Donnell K, Torre R, West C. Observations of second-harmonic generation from randomly rough metal surfaces. Phys Rev B 1997;55:7985–92.
[134] Butet JRM, Thyagarajan K, Martin OJ. Ultrasensitive optical shape characterization of gold nanoantennas using second harmonic generation. Nano Lett 2013;13:1787–92.
[135] Bautista G, Huttunen MJ, Maäkitalo J, Kontio JM, Simonen J, Kauranen M. Second-harmonic generation imaging of metal nano-objects with cylindrical vector beams. Nano Lett

2012;12:3207–12.
[136] Liz-Marzán LM. Tailoring surface plasmons through the morphology and assembly of metal nanoparticles. Langmuir 2006;22:32–41.
[137] Eustis S, El-Sayed MA. Why gold nanoparticles are more precious than pretty gold: noble metal surface plasmon resonance and its enhancement of the radiative and nonradiative properties of nanocrystals of different shapes. Chem Soc Rev 2006;35:209–17.
[138] Senapati D, Singh AK, Khan SA, Senapati T, Ray PC. Probing real time gold nanostar formation process using two-photon scattering spectroscopy. Chem Phys Lett 2011;504:46–51.
[139] Sauerbeck C, Haderlein M, Schürer B, Braunschweig BR, Peukert W, Klupp Taylor RN. Shedding light on the growth of gold nanoshells. ACS Nano 2014;8:3088–96.
[140] NicoloAccanto JB, Piatkowski L, Castro-Lopez M, Pastorelli F, Brinks D, van Hulst NF. Phase control of femtosecond pulses on the nanoscale using second harmonic nanoparticles. Light Sci Appl 2014;3:e143.
[141] Ray PC. Diagnostics of single base-mismatch DNA hybridization on gold nanoparticles by using the hyper-Rayleigh scattering technique. Angew Chem Int Ed 2006;45:1151–4.
[142] Neely A, Perry C, Varisli B, Singh AK, Arbneshi T, Senapati D, Kalluri JR, Ray PC. Ultrasensitive and highly selective detection of Alzheimer's disease biomarker using two-photon Rayleigh scattering properties of gold nanoparticle. ACS Nano 2009;3:2834–40.
[143] Kim Y, Johnson RC, Hupp JT. Gold nanoparticle-based sensing of "spectroscopically silent" heavy metal ions. Nano Lett 2001;1:165–7.
[144] Singh AK, Senapati D, Wang S, Griffin J, Neely A, Candice P, Naylor KM, Varisli B, Kalluri JR, Ray PC. Gold nanorod based selective identification of *Escherichia coli* bacteria using two-photon Rayleigh scattering spectroscopy. ACS Nano 2009;3:1906–12.
[145] Lu W, Arumugam SR, Senapati D, Singh AK, Arbneshi T, Khan SA, Yu H, Ray PC. Multifunctional oval-shaped gold-nanoparticle-based selective detection of breast cancer cells using simple colorimetric and highly sensitive two-photon scattering assay. ACS Nano 2010;4:1739–49.
[146] Abe A, Inoue K, Tanaka T, Kato J, Kajiyama N, Kawaguchi R, Tanaka S, Yoshiba M, Kohara M. Quantitation of hepatitis B virus genomic DNA by real-time detection PCR. J Clin Microbiol 1999;37:2899–903.
[147] Cao YC, Jin R, Mirkin CA. Nanoparticles with Raman spectroscopic fingerprints for DNA and RNA detection. Science 2002;297:1536–40.
[148] Wilcoxon J, Martin J, Parsapour F, Wiedenman B, Kelley D. Photoluminescence from nanosize gold clusters. J Chem Phys 1998;108:9137–43.
[149] Wang H, Huff TB, Zweifel DA, He W, Low PS, Wei A, Cheng J-X. *In vitro* and *in vivo* two-photon luminescence imaging of single gold nanorods. Proc Natl Acad Sci U S A 2005;102:15752–6.
[150] Mooradian A. Photoluminescence of metals. Phys Rev Lett 1969;22:185–7.
[151] Bouhelier A, Beversluis MR, Novotny L. Characterization of nanoplasmonic structures by locally excited photoluminescence. Appl Phys Lett 2003;83:5041–3.
[152] Drachev VP, Khaliullin E, Kim W, Alzoubi F, Rautian S, Safonov V, Armstrong R, Shalaev VM. Quantum size effect in two-photon excited luminescence from silver nanoparticles. Phys Rev B 2004;69:035318.
[153] Mohamed MB, Volkov V, Link S, El-Sayed MA. The lightning gold nanorods: fluorescence enhancement of over a million compared to the gold metal. Chem Phys Lett 2000;317:517–23.
[154] Deka G, Okano K, Masuhara H, Li Y-K, Kao F-J. Metabolic variation of HeLa cells migrating on microfabricated cytophilic channels studied by the fluorescence lifetime of NADH. RSC Adv 2014;4:44100–4.
[155] Deka G, Wu W-W, Kao F-J. *In vivo* wound healing diagnosis with second harmonic and fluorescence lifetime imaging. J Biomed Opt 2013;18:061222.
[156] Chu S-W, Chen S-Y, Tsai T-H, Liu T-M, Lin C-Y, Tsai H-J, Sun C-K. *In vivo* developmental biology study using noninvasive multi-harmonic generation microscopy. Opt Express 2003;11:3093–9.
[157] Boyd G, Yu Z, Shen Y. Photoinduced luminescence from the noble metals and its enhancement on roughened surfaces. Phys Rev B 1986;33:7923–36.
[158] Hao N-B, Lü M-H, Fan Y-H, Cao Y-L, Zhang Z-R, Yang S-M. Macrophages in tumor microenvironments and the progression of tumors. Clin Dev Immunol 2012;2012:948098.
[159] Fortunati I, Weber V, Giorgetti E, Ferrante C. Two-photon fluorescence correlation spectroscopy of gold nanoparticles under stationary and flow conditions. J Phys Chem C 2014;118:24081–90.
[160] Liu Y, Ashton JR, Moding EJ, Yuan H, Register JK, Fales AM, Choi J, Whitley MJ, Zhao X, Qi Y. A plasmonic gold nanostar theranostic probe for *in vivo* tumor imaging and photothermal therapy. Theranostics 2015;5:946–60.
[161] Farrer RA, Butterfield FL, Chen VW, Fourkas JT. Highly efficient multiphoton-absorption-induced luminescence from gold nanoparticles. Nano Lett 2005;5:1139–42.
[162] Eichelbaum M, Schmidt B, Ibrahim H, Rademann K. Three-photon-induced luminescence of gold nanoparticles embedded in and located on the surface of glassy nanolayers. Nanotechnology 2007;18:355702.
[163] Tong L, Cobley CM, Chen J, Xia Y, Cheng JX. Bright three-photon luminescence from gold/silver alloyed nanostructures for bioimaging with negligible photothermal toxicity. Angew Chem Int Ed 2010;49:3485–8.
[164] Howard SS, Straub A, Horton NG, Kobat D, Xu C. Frequency-multiplexed *in vivo* multiphoton phosphorescence lifetime microscopy. Nat Photon 2013;7:33–7.
[165] Hartland GV. Optical studies of dynamics in noble metal nanostructures. Chem Rev 2011;111:3858–87.
[166] de Abajo FJG. Graphene plasmonics: challenges and opportunities. ACS Photon 2014;1:135–52.
[167] Wang P, Slipchenko MN, Mitchell J, Yang C, Potma EO, Xu X, Cheng J-X. Far-field imaging of non-fluorescent species with subdiffraction resolution. Nat Photon 2013;7:449–53.
[168] Beversluis MR, Bouhelier A, Novotny L. Continuum generation from single gold nanostructures through near-field mediated intraband transitions. Phys Rev B 2003;68:115433.
[169] Talley CE, Jackson JB, Oubre C, Grady NK, Hollars CW, Lane SM, Huser TR, Nordlander P, Halas NJ. Surface-enhanced Raman scattering from individual Au nanoparticles and nano-

particle dimer substrates. Nano Lett 2005;5:1569–74.
[170] Huang X, El-Sayed IH, Qian W, El-Sayed MA. Cancer cell imaging and photothermal therapy in the near-infrared region by using gold nanorods. J Am Chem Soc 2006;128:2115–20.
[171] Jain PK, El-Sayed IH, El-Sayed MA. Au nanoparticles target cancer. Nano Today 2007;2:18–29.
[172] Sokolov K, Aaron J, Hsu B, Nida D, Gillenwater A, Follen M, MacAulay C, Adler-Storthz K, Korgel B, Descour M. Optical systems for *in vivo* molecular imaging of cancer. Technol Cancer Res Treat 2003;2:491–504.
[173] El-Sayed IH, Huang X, El-Sayed MA. Surface plasmon resonance scattering and absorption of anti-EGFR antibody conjugated gold nanoparticles in cancer diagnostics: applications in oral cancer. Nano Lett 2005;5:829–34.
[174] Hirsch LR, Stafford R, Bankson J, Sershen S, Rivera B, Price R, Hazle J, Halas N, West J. Nanoshell-mediated near-infrared thermal therapy of tumors under magnetic resonance guidance. Proc Natl Acad Sci USA 2003;100:13549–54.
[175] Betzig E, Patterson GH, Sougrat R, Lindwasser OW, Olenych S, Bonifacino JS, Davidson MW, Lippincott-Schwartz J, Hess HF. Imaging intracellular fluorescent proteins at nanometer resolution. Science 2006;313:1642–5.
[176] Hell SW. Far-field optical nanoscopy. Science 2007;316: 1153–8.
[177] Huang B, Wang WQ, Bates M, Zhuang XW. Three-dimensional super-resolution imaging by stochastic optical reconstruction microscopy. Science 2008;319:810–3.
[178] Heintzmann R, Jovin TM, Cremer C. Saturated patterned excitation microscopy – a concept for optical resolution improvement. J Opt Soc Am A Opt Image Sci Vis 2002;19:1599–609.
[179] Gustafsson MGL. Nonlinear structured-illumination microscopy: wide-field fluorescence imaging with theoretically unlimited resolution. Proc Natl Acad Sci USA 2005;102:13081–6.
[180] Fujita K, Kobayashi M, Kawano S, Yamanaka M, Kawata S. High-resolution confocal microscopy by saturated excitation of fluorescence. Phys Rev Lett 2007;99:228105.
[181] Rittweger E, Han KY, Irvine SE, Eggeling C, Hell SW. STED microscopy reveals crystal colour centres with nanometric resolution. Nat Photon 2009;3:144–7.
[182] Yamanaka M, Tzeng YK, Kawano S, Smith NI, Kawata S, Chang HC, Fujita K. SAX microscopy with fluorescent nanodiamond probes for high-resolution fluorescence imaging. Biomed Opt Express 2011;2:1946–54.
[183] Grotjohann T, Testa I, Leutenegger M, Bock H, Urban NT, Lavoie-Cardinal F, Willig KI, Eggeling C, Jakobs S, Hell SW. Diffraction-unlimited all-optical imaging and writing with a photochromic GFP. Nature 2011;478:204–8.
[184] Liberman V, Sworin M, Kingsborough RP, Geurtsen GP, Rothschild M. Nonlinear bleaching, absorption, and scattering of 532-nm-irradiated plasmonic nanoparticles. J Appl Phys 2013;113:053107.
[185] Chu SW, Wu HY, Huang YT, Su T, Lee H, Yonemaru Y, Yamanaka M, Oketani R, Kawata S, Shoji S, Fujita K. Saturation and reverse saturation of scattering in a single plasmonic nanoparticle. ACS Photon 2014;1:32–7.
[186] Chu S-W, Su T-Y, Oketani R, Huang Y-T, Wu H-Y, Yonemaru Y, Yamanaka M, Lee H, Zhuo G-Y, Lee M-Y. Measurement of a saturated emission of optical radiation from gold nanoparticles: application to an ultrahigh resolution microscope. Phys Rev Lett 2014;112:017402.
[187] Lee H, Oketani R, Huang Y-T, Li K-Y, Yonemaru Y, Yamanaka M, Kawata S, Fujita K, Chu S-W. Point spread function analysis with saturable and reverse saturable scattering. Opt Express 2014;22:26016–22.
[188] Wu H-Y, Huang Y-T, Shen P-T, Lee H, Oketani R, Yonemaru Y, Yamanaka M, Shoji S, Lin K-S, Chang C-W, Kawata S, Fujita K, Chu S-W. Ultrasmall all-optical plasmonic switch and its application to superresolution imaging. Sci Rep 2016;6:24293.
[189] Hoskins C, Min Y, Gueorguieva M, McDougall C, Volovick A, Prentice P, Wang Z, Melzer A, Cuschieri A, Wang L. Hybrid gold-iron oxide nanoparticles as a multifunctional platform for biomedical application. J Nanobiotechnol 2012;10:27.
[190] West PR, Ishii S, Naik GV, Emani NK, Shalaev VM, Boltasseva A. Searching for better plasmonic materials. Laser Photon Rev 2010;4:795–808.
[191] Saito T, Takahashi S, Obara T, Itabashi N, Imai K. Platinum plasmonic nanostructure arrays for massively parallel single-molecule detection based on enhanced fluorescence measurements. Nanotechnology 2011;22:445708.
[192] Chan GH, Zhao J, Hicks EM, Schatz GC, Van Duyne RP. Plasmonic properties of copper nanoparticles fabricated by nanosphere lithography. Nano Lett 2007;7:1947–52.
[193] Knight MW, King NS, Liu L, Everitt HO, Nordlander P, Halas NJ. Aluminum for plasmonics. ACS Nano 2013;8:834–40.
[194] Xu Z, Hou Y, Sun S. Magnetic core/shell Fe_3O_4/Au and Fe_3O_4/Au/Ag nanoparticles with tunable plasmonic properties. J Am Chem Soc 2007;129:8698–9.
[195] Garcia de Abajo FJ. Graphene plasmonics: challenges and opportunities. ACS Photon 2014;1:135–52.
[196] Raghunathan V, Han Y, Korth O, Ge N-H, Potma EO. Rapid vibrational imaging with sum frequency generation microscopy. Opt Lett 2011;36:3891–3.